

# Phenomenological study of solar-neutrino-induced $\beta\beta$ process of $^{100}\text{Mo}$

P. Domin<sup>a)</sup>, F. Šimkovic<sup>a)</sup>, S.V. Semenov<sup>b)</sup> and Yu.V. Gaponov<sup>b)</sup>

October 31, 2018

<sup>a)</sup>*Department of Nuclear Physics, Comenius University, SK-842 15 Bratislava,  
Slovakia*

<sup>b)</sup>*Russian Research Center "Kurchatov Institute", Moscow, Russia*

## Abstract

The detection of solar-neutrinos of different origin via induced  $\beta\beta$  process of  $^{100}\text{Mo}$  is investigated. The particular counting rates and energy distributions of emitted electrons are presented. A discussion in respect to solar-neutrino detector consisting of 10 tones of  $^{100}\text{Mo}$  is included. Both the cases of the standard solar model and neutrino oscillation scenarios are analyzed. Moreover, new  $\beta^-\beta^+$  and  $\beta^-/EC$  channels of the double-beta process are introduced and possibilities of their experimental observation are addressed.

## 1 Introduction

The nature and the masses of the neutrinos has not yet been established phenomenologically [1]. The problem of the neutrino mass scale can be solved only by combining the neutrino oscillation data with the phenomenology of neutrinoless double-beta decay ( $0\nu\beta\beta$  decay).

The observed fluxes of solar neutrinos are much reduced compared with theoretical predictions based on the standard solar model (SSM) [2]. It has been confirmed in different solar-neutrino experiments: Homestake [3], Kamiokande [4], SAGE [5], GALLEX [6], and Super-Kamiokande [7]. Recently announced result by the Sudbury Neutrino Observatory (SNO) has shown clear indication of neutrino oscillation [8], i.e., of beyond standard model physics. In particular, there is a strong evidence that  $\nu_e$  from the sun are converted to  $\nu_\mu$  or  $\nu_\tau$ .

The great challenge of solar-neutrino research is to make accurate measurements of neutrinos with energy less than 1 MeV. We remind that more than 98% of the calculated solar-neutrino flux lies in this energy region. Especially, the pp neutrinos represent the dominant mode of neutrino emission from the sun. It is worthwhile to notice that the prediction of the pp neutrino flux is almost solar-model independent. New generation of low threshold solar-neutrino experiments are in preparation (BOREXINO) or under consideration (GENIUS, HERON, HELLAZ, LENS, MOON, XMASS ...). The measurements of the total flux, flavor content,

energy spectrum, and time dependence of the fundamental neutrinos are planned by using advantage of detection both charged and neutral weak currents as well as of the neutrino-electron scattering.

In the framework of some of future experiments (GENIUS, MOON, XMASS) simultaneous spectroscopic studies of the  $0\nu\beta\beta$  decay and study of low energy solar neutrinos will be performed. In the MOON detector with 10 tons of  $^{100}\text{Mo}$  solar neutrinos are proposed to be detected by inverse  $\beta$  decay [9]. We note that  $^{100}\text{Mo}$  is suitable for charge current registration of solar neutrinos due to low threshold of 0.168 MeV, what allows observation of low energy pp neutrinos.

In this contribution we analyze the possibility of detection of solar neutrinos via neutrino-induced double-beta process ( $\beta\beta$ -process) of  $^{100}\text{Mo}$ . We note that the  $\beta\beta$  process induced by neutrinos was discussed for the first time in connection with detection of reactor neutrinos and artificial sources in Refs. [10, 11]. Here, we present the predictions for the solar neutrinos absorption rates by assuming the standard solar model and different neutrino oscillation scenarios. The subject of our interest is also the background coming from the two-neutrino double-beta decay of  $^{100}\text{Mo}$  in registration of solar neutrinos of different origin. Finally, new modes of induced  $\beta\beta$  process,  $\beta^-\beta^+$  and  $\beta^-/EC$  channels, are introduced and discussed.

## 2 Cross-section of the neutrino induced $\beta\beta$ process

The neutrino induced double-beta transition (induced  $\beta\beta$  transition) [10],

$$\nu_e + (A, Z) \rightarrow (A, Z + 2) + 2e^- + \bar{\nu}_e, \quad (1)$$

is a reaction allowed within the Standard model. It is a second order process in the weak interaction, observation of which by the help of reactor-neutrino flux has been found possible due to resonant enhancement of the corresponding amplitude depending on the width of the intermediate nuclear state [11]. Below, we briefly present the theory of the induced  $\beta\beta$  process concerning ground state to ground state nuclear transition.

The differential cross section of the induced  $\beta\beta$  process can be written as

$$\frac{d\sigma(\varepsilon_\nu)}{d\varepsilon_1 d\varepsilon_2} = \frac{(G_\beta)^4 g_A^4 m_e^4}{8\pi^5} \pi_1 \varepsilon_1 F(\varepsilon_1, Z_f) \pi_2 \varepsilon_2 F(\varepsilon_2, Z_f) (w_0 - \varepsilon_1 - \varepsilon_2 + \varepsilon_\nu)^2 K_{GT} \quad (2)$$

with  $\pi_k = p_k/m_e$ ,  $\varepsilon_k = E_k/m_e$  ( $k = 1, 2$ ) and  $\varepsilon_\nu = E_\nu/m_e$ .  $p_k$  and  $E_k$  are momenta and energies of electrons, respectively.  $E_\nu$  denotes energy of the incident neutrino.  $F(\varepsilon_1, Z_f)$  is Coulomb correction factor,  $w_0$  is the energy difference of the target and final nuclei in units of electron mass. Factor  $K_{GT}$  containing the energy denominators is given by

$$K_{GT} = \frac{3}{4} \left( \left| \sum_m (K_m + L_m) \right|^2 + \frac{1}{3} \left| \sum_m (K_m - L_m) \right|^2 \right) \quad (3)$$

with

$$K_m = \left[ (\varepsilon_m + \frac{1}{2}i\gamma_m - \varepsilon_i + \varepsilon_1 - \varepsilon_\nu)^{-1} + (\varepsilon_m + \frac{1}{2}i\gamma_m - \varepsilon_i + \varepsilon_2 + \varepsilon_{\bar{\nu}_2})^{-1} \right]$$

$$\begin{aligned}
& \times \langle 0_{g.s.}^+, f | \sum_i \tau_i^+ \vec{\sigma}_i | 1_m^+ \rangle \langle 1_m^+ | \sum_i \tau_i^+ \vec{\sigma}_i | 0_{g.s.}^+, i \rangle, \\
L_m &= \left[ (\varepsilon_m + \frac{1}{2}i\gamma_m - \varepsilon_i + \varepsilon_1 + \varepsilon_{\bar{\nu}_2})^{-1} + (\varepsilon_m + \frac{1}{2}i\gamma_m - \varepsilon_i + \varepsilon_2 - \varepsilon_{\nu})^{-1} \right] \\
& \times \langle 0_{g.s.}^+, f | \sum_i \tau_i^+ \vec{\sigma}_i | 1_m^+ \rangle \langle 1_m^+ | \sum_i \tau_i^+ \vec{\sigma}_i | 0_{g.s.}^+, i \rangle. \tag{4}
\end{aligned}$$

Here,  $\varepsilon_m = E_m/m_e$  and  $\gamma_m = \Gamma_m/m_e$ .  $E_m$  and  $\Gamma_m$  are energy and width of the  $m$ -th  $1^+$  intermediate nuclear state, respectively.  $\varepsilon_{\bar{\nu}_2}$  is the energy of outgoing entineutrino in unit of  $m_e$ .  $|0_{g.s.}^+, i\rangle$ ,  $|0_{g.s.}^+, f\rangle$  and  $|1_m^+\rangle$  denote wave functions of initial, final and intermediate nuclear states, respectively.

The factors  $K_m$  and  $L_m$  are similar to those entering the expression for two-neutrino double-beta decay ( $2\nu\beta\beta$  decay) amplitude with one important difference. The sign in front of the energy of incoming neutrino is changed to minus. Than two of four denominators in Eq. (4) exhibit singular behavior if the incident neutrino energy is larger than the threshold for creation of a real state of the intermediate nucleus

$$\varepsilon_{\nu} > 1 + \varepsilon_m - \varepsilon_i, \quad (m < m^{RS}). \tag{5}$$

$\varepsilon_{m^{RS}}$  denotes the energy of highest lying excited state of the intermediate nucleus satisfying relation (5).

The total cross-section is calculated by keeping in mind that widths of low lying states of the intermediate nucleus are very small in comparision with their energies due to electromagnetic and weak decay channels. After performing integration over the energies of outgoing electrons in Eq. (2), we obtain

$$\begin{aligned}
\sigma(\varepsilon_{\nu}) &= \frac{(G_{\beta})^4 g_A^4 m_e^6}{2\pi^4} \sum_{m=0}^{m^{RS}} \left| \langle 0_{g.s.}^+, f | \sum_i \tau_i^+ \vec{\sigma}_i | 1_m^+ \rangle \langle 1_m^+ | \sum_i \tau_i^+ \vec{\sigma}_i | 0_{g.s.}^+, i \rangle \right|^2 \\
&\times \frac{1}{\gamma_m} \pi_r^{(m)} \varepsilon_r^{(m)} F(Z_f, \varepsilon_r^{(m)}) \int_1^{\varepsilon_m - \varepsilon_f} d\varepsilon_2 \pi_2 \varepsilon_2 F(Z_f, \varepsilon_2) (\varepsilon_m - \varepsilon_f - \varepsilon_2)^2, \tag{6}
\end{aligned}$$

where  $\varepsilon_r^{(m)} = \varepsilon_{\nu} - \varepsilon_m + \varepsilon_i$ . We note that the dominant contribution to the cross-section comes from the transitions through the real states of the intermediate nucleus ( $m < m^{RS}$ ) and that contribution of transitions through virtual intermediate states (like in  $2\nu\beta\beta$  decay) is negligible (suppressed by factor  $\sim \gamma_m$ ).

Next, we introduce the partial width  $\gamma_{mf}$  of  $m$ -th state of the intermediate nucleus associated with the  $\beta^-$  transition to the ground state of final nucleus. We have

$$\gamma_{mf} = \frac{(G_{\beta})^2 g_A^2 m_e^4}{2\pi^3} \left| \langle 0_{g.s.}^+, f | \sum_i \tau_i^+ \vec{\sigma}_i | 1_m^+ \rangle \right|^2 \int_1^{\varepsilon_m - \varepsilon_f} d\varepsilon_2 \pi_2 \varepsilon_2 F(Z_f, \varepsilon_2) (\varepsilon_{m_0} - \varepsilon_f - \varepsilon_2)^2. \tag{7}$$

It allows us to write the total cross-section of the neutrino-induced  $\beta\beta$ -process in a compact form

$$\sigma(\varepsilon_{\nu}) = \sum_{m=0}^{m^{RS}} \sigma_{\beta}^{(m)}(\varepsilon_{\nu}) \frac{\gamma_{mf}}{\gamma_m}, \tag{8}$$

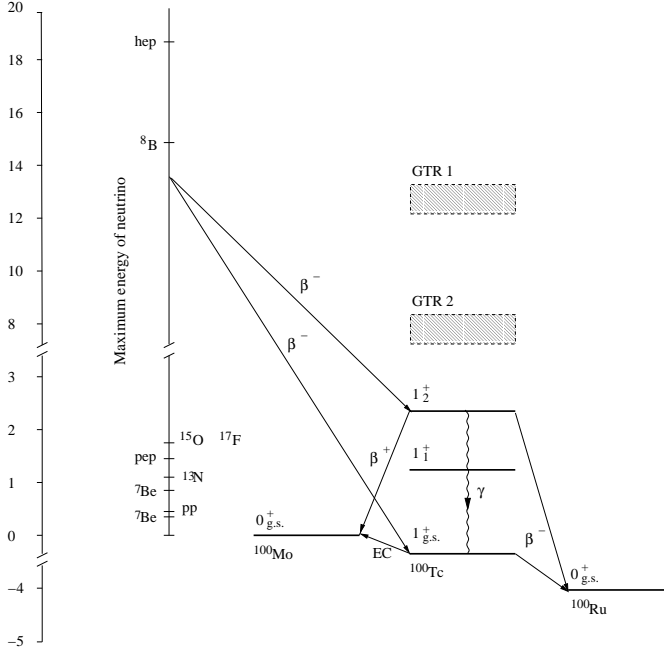


Figure 1: Nuclear level and transition schemes  $^{100}\text{Mo}$  for  $\beta\beta$  processes induced by solar neutrino absorption. GTR1 and GTR2 denote giant Gamow-Teller resonances. The energy scale is in units of MeV.

where  $\sigma_\beta^{(m)}(\varepsilon_\nu)$  represents the cross-section of the neutrino-induced single- $\beta$  decay from the ground state of the initial nucleus to the  $m$ -th state of the intermediate nucleus:

$$\sigma_\beta^{(m)}(\varepsilon_\nu) = \frac{(G_\beta)^2 g_A^2 m_e^2}{\pi} \left| \langle 1_m^+ | \sum_i \tau_i^+ \vec{\sigma}_i | 0_{g.s.}^+, i \rangle \right|^2 \pi_r^{(m)} \varepsilon_r^{(m)} F(Z_f, \varepsilon_r^{(m)}). \quad (9)$$

The total width  $\gamma_m$  of the  $m$ -th excited state of the intermediate nucleus is much larger as the partial  $\beta$  width  $\gamma_{mf}$  due to preferably electromagnetic deexcitation to lower lying states. However, in the case of ground state of the intermediate nucleus there is a different situation, in particular  $\gamma_{mf}/\gamma_m \approx 1$ . Thus the transition through the lowest state of the intermediate nucleus gives the dominant contribution to the total cross section of the induced  $\beta\beta$  process (see Eq. (8)). We note that a different situation can be in case of the neutrino-induced  $\beta\beta$  process with emission of  $\gamma$ -ray, which has origin in electromagnetic deexcitation of levels of the intermediate nucleus. The details of this process we expect to discuss in next publication.

From the above study it follows that electrons emitted in the neutrino-induced  $\beta\beta$  process exhibit different behavior from those in the  $2\nu\beta\beta$  decay, which is considered to be the major background in some of planned solar-neutrino detectors. The induced  $\beta\beta$  transition can be to a good approximation considered as two subsequent independent processes (see Eq. (8)) the induced single- $\beta^-$  transition to the

Table 1: Solar neutrino signal rates per day in 10 tones of  $^{100}\text{Mo}$  for transition through ground state as well as excited states of intermediate  $^{100}\text{Tc}$ . B(GT) and  $E^*$  denote the Gamow-Teller strength and the excitation energy, respectively.

state:	$1_{g.s.}^+$	$1_1^+$	$1_2^+$	GTR1	GTR2
$B(\text{GT})$ :	0.33	0.13	0.23	23.1	2.9
$E^*(\text{MeV})$ :	0	1.4	2.6	13.3	8.0
source	Production rate in 10 tones of $^{100}\text{Mo}$ per day				
pp	3.4	-	-	-	-
pep	$7.1 \cdot 10^{-2}$	-	-	-	-
$^7\text{Be}(1)$	0.04	-	-	-	-
$^7\text{Be}(2)$	1.0	-	-	-	-
$^8\text{B}$	0.04	0.01	0.01	$1.4 \cdot 10^{-4}$	0.01
hep	$3.1 \cdot 10^{-5}$	$9.6 \cdot 10^{-6}$	$1.3 \cdot 10^{-5}$	$2.1 \cdot 10^{-5}$	$3.8 \cdot 10^{-5}$
$^{13}\text{N}$	0.11	-	-	-	-
$^{15}\text{O}$	0.16	$5.1 \cdot 10^{-4}$	-	-	-
$^{17}\text{F}$	$1.96 \cdot 10^{-3}$	$6.4 \cdot 10^{-6}$	-	-	-

ground state of intermediate nucleus followed by nuclear  $\beta^-$  decay to the ground state of final nucleus. The time delay between both  $\beta$  processes is about 20 second for  $A=100$  system. It is worthwhile to notice that in the  $2\nu\beta\beta$  decay electrons are emitted simultaneously. In addition, they are strongly correlated what allows to eliminate  $2\nu\beta\beta$  decay background through coincidence measurements.

### 3 Solar neutrino absorption rates for $^{100}\text{Mo}$

The solar neutrino absorption rates for  $^{100}\text{Mo}$  are important in the evaluation of detector for planned MOON experiment. In this section we present complementary and more detailed calculations to those of Ref. [9].

The absorption rate of solar neutrinos from the source  $s$  is given by [2, 12]

$$R_\nu = \int \sigma(\varepsilon_\nu) \rho_s(\varepsilon_\nu) d\varepsilon_\nu. \quad (10)$$

Here,  $\rho_s(\varepsilon_\nu)$  is the spectrum of incident solar-neutrino flux. The total cross-section  $\sigma(\varepsilon_\nu)$  of the neutrino-induced  $\beta\beta$  process is given in Eq. (8).

The nuclear level scheme for solar-neutrino-induced  $\beta\beta$ -transition of  $^{100}\text{Mo}$  is presented in Fig. 1. The dominant nuclear transitions are realized through  $1^+$  states of the intermediate nucleus. The corresponding Gamow-Teller strengths have been determined experimentally by measuring the electron capture and  $\beta$ -decay rates of  $^{100}\text{Tc}$  ( $\log ft_\beta = 4.60$ ) [13] as well as of cross-section of the  $^{100}\text{Mo}(^3\text{He}, t)^{100}\text{Tc}$  reaction [14].

In Table (1) we present solar-neutrino signal rates per day in 10 tones of  $^{100}\text{Mo}$ , assuming there are no oscillations of neutrinos. We note that transitions through higher excited states of the intermediate nucleus are strongly suppressed. There

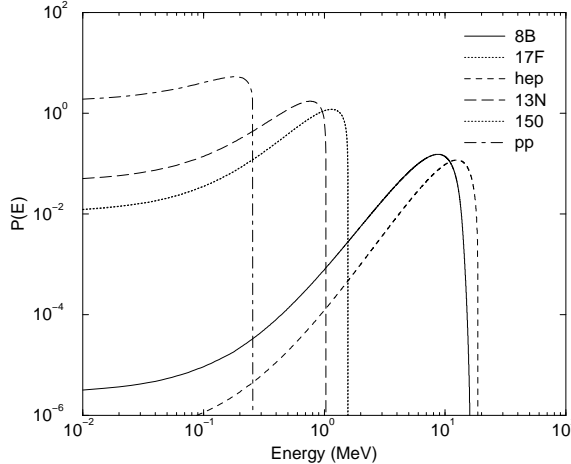


Figure 2: Probability density of the emission of the single electron via solar-neutrino-induced inverse  $\beta\beta$  decay on  $^{100}\text{Mo}$ .

Table 2: Particular solar-neutrino capture rates in unit of SNU (solar-neutrino unit) for  $^{100}\text{Mo}$ ,  $^{37}\text{Cl}$  and  $^{71}\text{Ga}$ . Contributions coming only from the dominant transition through the ground state of the intermediate nucleus  $^{100}\text{Tc}$  were taken into account.

source	$pp$	$pep$	$^7\text{Be}$	$^8\text{B}$	$hep$	$^{13}\text{N}$	$^{15}\text{O}$	$^{17}\text{F}$
$^{100}\text{Mo}$	652	13.6	197	7.8	0.01	22	31.6	0.38
$^{37}\text{Cl}$	0	0.22	1.15	5.76	0.04	0.09	0.33	0.0
$^{71}\text{Ga}$	69.7	2.8	34.2	12.1	0.1	3.4	5.5	0.1

transitions were estimated by assuming  $\gamma$ -deexcitation to the ground state of the intermediate nucleus. We remind that neutrino-induced  $\beta\beta$  transition through excited intermediate states (without accompanying  $\gamma$ -ray emission) is strongly suppressed due to small ratio  $\gamma_{mf}/\gamma_m$ .

In calculation we used energy distribution of solar neutrinos predicted by the standard solar model [2, 12]. The probability density for emission of single electron of given energy induced by solar neutrinos of a given source is plotted in Fig. (2). The solar-neutrino absorption rate for  $^{100}\text{Mo}$  is compared with those for  $^{37}\text{Cl}$  and  $^{71}\text{Ga}$  isotopes (see Table 2). We note that detector built of  $^{100}\text{Mo}$  isotope allows to register significantly larger amount of solar neutrinos as it is in the case of  $^{37}\text{Cl}$  and  $^{71}\text{Ga}$ . It is due to lower threshold for solar-neutrino absorption by this isotope. The relevant thresholds for  $^{100}\text{Mo}$ ,  $^{37}\text{Cl}$  and  $^{71}\text{Ga}$  targets are 0.168 MeV, 0.817 MeV and 0.235 MeV, respectively.

It is worthwhile to notice that there are also other standard model allowed channels of the neutrino-induced  $\beta\beta$ -transition ( $\beta^-/EC$  and  $\beta^-/\beta^+$  modes), which

Table 3: The solar neutrino absorption rates in  $^{100}\text{Mo}$  in SNU. The standard solar model (SSM) predictions are compared with those of three MSW and one vacuum oscillation solutions of the solar neutrino problem [15]. SMA, LMA, LOW and VO stand for the small mixing angle, the large mixing angle, the low  $\Delta m^2$  and vacuum oscillations solutions, respectively.

source	pep	$^7\text{Be}(1)$	$^7\text{Be}(2)$	pp	$^8\text{B}$	$^{13}\text{N}$	$^{15}\text{O}$	$^{17}\text{F}$
SSM	14	0.81	197	652	7.8	22	32	0.38
SMA	0.05	0.41	0.58	540	2.9	1.09	0.50	0.01
LMA	4.97	0.45	90	372	2.19	10	13	0.15
LOW	6.00	0.44	94	351	3.18	11	14	0.17
VO	0.5	0.55	162	100	0.63	3	6	0.07

have been not discussed in literature yet. For  $^{100}\text{Mo}$  target they are given by

$$\begin{aligned} \nu_e + {}^{100}\text{Mo} &\rightarrow {}^{100}\text{Mo} + e^- + e^+ + \nu_e \quad (\beta^-/\text{EC}), \\ \nu_e + e^- + {}^{100}\text{Mo} &\rightarrow {}^{100}\text{Mo} + e^- + \nu_e \quad (\beta^-\beta^+). \end{aligned} \quad (11)$$

The corresponding cross-sections of these reactions can be calculated by omitting the term  $L_m$  in Eqs. (2), (3) and (4). In addition, in the case of  $\beta^-/\text{EC}$  mode one has to replace  $\varepsilon_2$  with  $-1$  and to modify appropriate the normalization of one electron. The cross-sections of these modes are of the form given in Eq. (8), however,  $\gamma_{mf}$  represents the partial width of  $m$ -th intermediate  $1^+$  state of  $^{100}\text{Tc}$  in respect to  $\beta^+$  or  $\text{EC}$  decay channels. For the ground state of  $^{100}\text{Tc}$  we have:  $\gamma_{mf}/\gamma_m = 0.0018$  ( $\text{EC}$ ),  $0$  ( $\beta^+$ ). Thus,  $\beta^-/\text{EC}$  mode is suppressed in comparison with the  $\beta^-\beta^-$  one by about of three orders of magnitude. In the case of pp solar neutrinos the corresponding absorption rate is 1.2 SNU (2.3 events per year in 10 tones of  $^{100}\text{Mo}$ ). The  $\beta^-\beta^+$  mode is undetectable for this type of detector.

Nowadays, we have a strong indication in favor of solar neutrino oscillations coming from SNO experiment [8]. There are different scenarios for mixing of neutrinos, which differ very little in their predictions. Usually, one vacuum oscillation solution and three MSW solutions of the deficit of solar neutrino events are considered. They are the Small Mixing Angle, the Large Mixing Angle, the LOW  $\Delta m^2$  solutions. In Table 3 we discuss the solar neutrino deficit assuming SMA, LMA, LOW and vacuum oscillation schemes for neutrinos of different origin. We notice that LMA and LOW solar neutrino absorption rates are close each to other for all types of neutrinos. The SMA solution offers considerably smaller values especially in the case of pp, pep and  $^7\text{Be}$  neutrinos.

## 4 Conclusions

The solar-neutrino anomaly is a controversial problem, which attracts attention of both theoreticians and experimentalists for a long time. New experimental data and

theoretical ingredients have to be merge to give reliable predictions for oscillation parameters.

In this contribution the charged current solar neutrino absorption is discussed in context of the neutrino-induced  $\beta\beta$  process. We have shown that to a good approximation, this process can be considered as neutrino-induced  $\beta$ -decay followed by single- $\beta$  decay. This fact allows to identify clearly the  $2\nu\beta\beta$  decay background in planned solar neutrino experiments.

Moreover, complementary theoretical study in respect to the MOON project is presented. Solar-neutrino absorption rates are calculated by assuming SSM neutrino flux spectrum. The probability density for emission of single electron is evaluated. A comparison of the SSM prediction for absorption of neutrinos in  $^{100}\text{Mo}$  is compared with those of most favored neutrino oscillation scenarios.

## References

- [1] S. M. Bilenky, C. Giunti and W. Grimus, *Prog. Part. Nucl. Phys.* **45** (1999) 1.
- [2] J. N. Bahcall, S. Basu and M. H. Pinsonneault, *Phys. Lett. B* **433** (1998) 1.
- [3] R. Davis Jr., *Prog. Part. Nucl. Phys.* **32** (1994) 13.
- [4] Kamiokande Collaboration, Y Fukuda et al., *Phys. Rev. Lett.*, **77** (1996) 1683.
- [5] SAGE collaboration, A. I. Abazov et al., *Phys. Rev. Lett.* **67** (1991) 3332; D. N. Abdurashitov et al., *Phys. Rev. Lett.* **77** (1996) 4708.
- [6] GALLEX collaboration, P. Anselmann et al., *Phys. Lett. B* **285** (1992) 376; W. Hampel et al., *Phys. Lett. B* **388** (1996) 384.
- [7] Super-Kamiokande Coll., S. Fukuda *et al.*, *Phys. Rev. Lett.* **86** (2001) 5651.
- [8] SNO Collaboration, Q.R. Ahmad et. al., *Phys. Rev. Lett.* **87** (2001) 071301.
- [9] H. Ejiri et al., *Phys. Rev. Lett.* **85** 2917 (2000); H. Ejiri, *Phys. Rep.* **338** (2000) 265.
- [10] S. V. Semenov, Yu. V. Gaponov and R. U. Khafizov, *Yad. Fiz.* **61** (1998) 1379.
- [11] L. V. Inzhechik, Yu. V. Gaponov and S. V. Semenov, *Yad. Fiz.* **61** (1998) 1384.
- [12] <http://www.sns.ias.edu/~jnb>.
- [13] B. Singh et al., *Nucl. Data. Sheets* **84** (1998) 478.
- [14] H. Akimune et al., *Phys. Lett. B* **394** (1997) 23.
- [15] J. N. Bahcall, P. I. Krastev, and A. Yu. Smirnov, *Phys. Rev. D* **58** (1998) 096016.